Silver and Silver-Iron Nanoparticles Synthesized by Photoreduction for Applications in Cancer Therapy

Karina de Oliveira Gonçalves
Departamento de Física
Universidade Federal de São Paulo
Diadema, Brazil
kgoncalves@unifesp.br

Fúlvio Corazza
Biotechnology Center
Institute of Energy and Nuclear Research
São Paulo, Brazil
fcfulviocorazza@gmail.com

Daniel Perez Vieira
Biotechnology Center
Institute of Energy and Nuclear Research
São Paulo, Brazil
dpvieira@ipen.br

Lilia Coronato Courrol
Departamento de Física
Universidade Federal de São Paulo
Diadema, Brazil
lccourrol@gmail.com

***Abstract*— Metal nanoparticles have been extensively studied for various purposes including therapeutic applications for cancer. In this study, nanoparticles of silver and silver-iron with aminolevulinic acid (ALA) were synthesized using (ALA:AgNPs and ALA:AgFeNPs) the photoreduction method with a 300 W xenon lamp, characterized by UV/vis absorption, zeta potential, x-rays diffraction, FTIR and transmission electron microscopy. The sizes obtained were ~ 23 nm for silver and ~ 12 nm for iron. Cytotoxicity assays were performed on breast tumor cells (MCF-7) and prostate cancer cells (LNCaP). The results obtained showed that it was possible to synthesize silver and silver-iron nanoparticles by the photoreduction method, and to functionalize their surfaces with ALA, which was delivered to the cells and converted to protoporphyrin IX (PpIX).**

Keywords*— *silver nanoparticles, iron nanoparticles, photoreduction, cancer

Introduction

Silver nanoparticles (AgNPs) attract significant interest because of their applicability in various areas [1]. The antimicrobial properties of AgNPs demonstrate efficiency against more than 650 pathogenic organisms, making these nanostructures applicable to products in the medical-hospital area (tissues and implants), shoes and sneakers, food storage containers, washing machines and air conditioners [2,3]. In biological systems, silver nanoparticles can cause the production of reactive oxygen species, changes in the cell cycle, damage to the genetic material, inflammatory processes and cell death [4]. In a study published by Asharani et al (2009), the toxicity of silver nanoparticles was tested in human lung fibroblasts and human glioblastoma cells [5]. The results showed the presence of AgNPs in the nucleus and in the mitochondria, which indicated a rupture of the mitochondrial respiratory chain originating reactive oxygen species (ROS) and blockage of ATP synthesis causing DNA damage. Generation of ROS is also known to induce apoptosis/cell death in various cell culture models [6].

Silver nanoparticles have applications in cancer treatment and are drug transporters that can deliver therapeutic agents. [7].

Aminolevulinic acid (ALA) is the first metabolite in the heme biosynthesis pathway. Porphyrins are biosynthesized from aminolevulinic acid (ALA). Moan et. al [8] showed enhanced ALA-mediated protoporphyrin IX (PpIX) accumulation in tumor cells and effective cell destruction after light illumination.

The objective of this study was to synthesize metallic nanoparticles (silver and iron) by the photoreduction method, and at the same time functionalize the surfaces with aminolevulinic acid (ALA), improving the delivery of the drug, and increasing the cytotoxic effects on tumor cells [9].

I. Materials and Methods

A. Silver and silver-iron nanoparticles with 5-ALA

To prepare ALA:AgNPs, 45 mg de $AgNO_3$ were mixed with 13.5 mg de ALA and 30 mg of polyethylene glycol (PEG) in 30 mL of distilled water at 20ºC. The process was accompanied by vigorous stirring for 5 minutes, and 10 mL of the resulting solution was exposed to a 300 W xenon lamp for 1 minute. After irradiation pH solution was adjusted to ~ 7.0.

To prepare ALA:AgFeNPs, 45 mg of iron powderwere diluted in 30 mL of distilled water and the pH solution was adjusted to 12. After that, 45 mg of $AgNO_3$, 13.5 mg of ALA and 30 mg of PEG were added in solution, homogenized for 5 minutes and then exposed to a 300 W xenon lamp for 1 minute. After irradiation, the pH solution was adjusted to ~ 7.

B. Characterization

The UV-vis absorption spectra were measured by a Shimatzu spectrophotometer, using 1-cm quartz cells. The shape and sizes of ALA:AgNPs and ALA:AgFeNPs were obtained from transmission electron microscope (TEM) a Jeol (Zeiss, Germany). The effective surface charges on the ALA:AgNPs and ALA:AgFeNPs were measured using zeta potential (Malvern Instruments Zetasizer, Worcestershire, UK).

The structural identification of the ALA:AgFeNPs sample was performed using the X-ray diffraction analysis (XRD) measurement using a Bruker D8 Advance 3kW diffractometer (Cu radiation tube, 250 mm goniometer, 40 kV, 30 mA) at Multiuser Center of the Nuclear Fuel (IPEN/CNEN-SP). The technique was performed for silver-iron nanoparticles. The material was separated using a

Foundation Research Support of the State of São Paulo (FAPESP) and CAPES.

magnet. The supernatant was then centrifuged for 5 minutes at 10,000 rpm, always separating the supernatant from the bottom body, and centrifuging the supernatant again. The process was repeated 5 times, and the contents obtained were oven dried (60°C) for 24 hours. The spectra were analyzed using Qualx2 software.

Peaks were compared to the compounds databases of software to make assumptions between obtained Crystal diffraction spectra versus used those from known compounds. The full width at half maximum of peaks (FWHM) values was used to crystallite size calculations through Scherrer's calculation (λ=0.154056, K=0.91).

C. Cell Culture

Two tumor lines were evaluated: breast cancer cells MCF-7 (**ATCC**® HTB22™) and human prostate cancer cells LNCaP (**ATCC**®. CRL1740™). The cells were maintained in RPMI 1640 medium supplemented with 10% fetal bovine serum (FBS) and 1% penicillin/streptomycin at 37 °C with 5% CO_2. The cells were routinely subcultures every 3 days with 70-80% confluency and harvested using 0.25% trypsin.

D. Cell Viability

Cells ($8x10^3$ cells/well) were plated on 96-well flat bottom plates. After 24 hours, the cells were incubated with dilutions of the test compound (ALA:AgNPs and ALA:AgFeNPs) at the concentrations of 5, 10, 20, 30 and 40 mL diluted in RPMI medium to a final volume of 500 µL. The plates were then incubated for 24 hours at 37 ° C and 5% CO_2 atmosphere. Subsequently, the supernatant was removed, and the cells were washed with PBS and the cells were incubated for 24 hours with RPMI medium. Cell viability was evaluated by MTS (CellTiter 96® AQueous MTS Reagent) in formazan. The amount of product is absorbable at 490 nm and is directly proportional to the number of live cells in culture. The results were statistically compared (ANOVA and Dunnett test) or negative (control cells, NaCl 0.9%) or positive (suspension of latex powder, 0.5 g/L).

II. Results and Discussion

A. Silver and silver-iron nanoparticles characterization

The absorbance spectra of the nanoparticles are shown in Fig. 1, where the characteristic band of silver nanoparticles (~ 420 nm) appears due to the SPR (surface plasmon resonance) effect, indicating the formation of silver nanoparticles. Not all metals have plasmon resonanc because it is necessary for the presence of free conduction electrons, and thus the iron does not present distinguishab bands in the region of the observed spectrum.

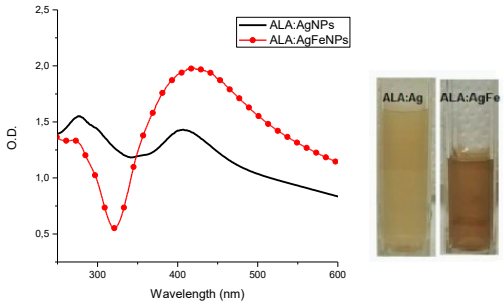

Fig. 1. Absorption spectra of ALA:AgNPs and ALA:AgFeNPs (pH ~7.0).

The silver and silver iron nanoparticles were synthesized by the photoreduction method with the use of a Xenon lamp. White light lighting was essential for the formation of nanoparticles, heating and supplying photons to the solution. The light still interacts with ALA, which has a low pKa value (4.05), releases more H^+ ions. In this way the light irradiation acts as a catalyst for the metal reduction (oxidation / photoinduced reduction), providing ions that culminate in the passage of the silver from the valence 1^+ to zero, and therefore they were different for each material. The elevation of temperature promoted by the irradiation also plays an important role in the synthesis process [10].

The result obtained with the X-ray (XRD) shows the reflections referring to the interplanar distances characteristic of the crystalline phases of the magnetite and silver [11].

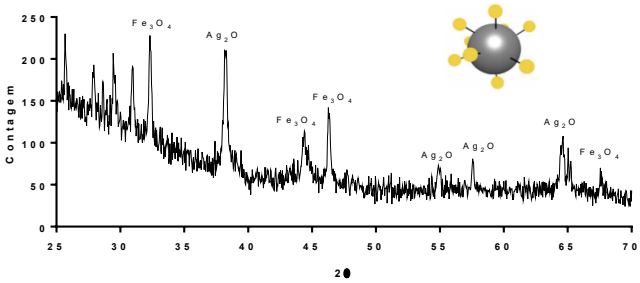

Fig. 2. X-ray diffraction spectra of silver-iron particles (ALA:AgFeNPs - 2 minutes of illumination - pH 7.0) and the powders obtained after centrifugation and drying of the sample (10.000 rpm for 5 minutes and drying at 60 ° C for 24 hours)

Using the Scherrer equation and the values of the width at half height of the most intense magnetite and silver peak, considering λ=1.54056, it was possible to calculate the crystallite size (Eq.1).

$$Z_c = 0{,}9\ .\lambda\ /B.\ cos\theta \qquad (1)$$

The diameter obtained for the silver was 12 nm and for the magnetite, it was 23 nm, which confirms the results obtained by transmission electron microscopy (MTEM), with smaller particles for silver and larger for iron. It is possible to note in Fig. 3a that the solutions of ALA:AgNPs are quite heterogeneous with portions of very large particles and portions of very small particles. Figure 3b shows greater homogeneity for the ALA:AgFeNPs samples.

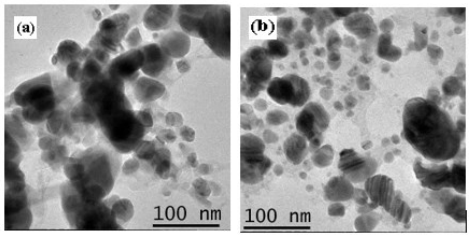

Fig. 3. TEM image of the samples: (a) ALA:AgNPs and (b) ALA:AgFeNPs, with the lower contrast nanoparticles are like silver with ~ 12 nm and the larger ones with iron with ~ 23 nm.

Table 1 presents the obtained values of zeta potential and polydispersity index, indicating moderate solution stability [10, 11].

TABLE I. SIZE, ZETA POTENCTIAL AND POLYDISPERSITY INDEX OF SILVER AND SILVER-IRON NANOPARTICLES.

	Zeta Potential (mV)	*PDI*	*Hydrodinamic diameter (nm)*
ALA:AgNPs	-36.6 ± 8.45	0.319	77.02
ALA:AgFeNPs	-30.8 ± 4.40	0.336	3296

FTIR spectra showed different bands for silver and silver-iron. The two nanoparticles show some bands in the same regions (Fig. 4): ~ 2880 cm $^{-1}$ (C-H) and ~ 1110 cm $^{-1}$ (C-H). The C = O band of the carboxyl (~ 1716 cm $^{-1}$), which for ALA was strong, decreases and suggests the interaction of the nanoparticles with the functional group.

The reaction pH of the nanoparticles around 3.4 favors the binding of the carboxyl group (pKa 4.05) with the metal ions Ag^{+}.

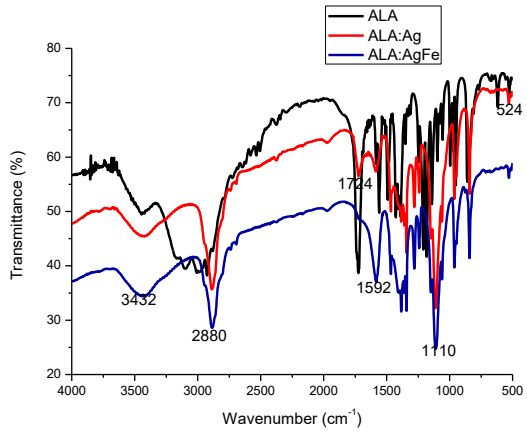

Fig. 4. FTIR spectra of the nanoparticles: spectrum of ALA, ALA:AgNPs and ALA:AgFeNPs and their respective functional groups.

Cytotoxic assays of silver and silver-iron nanoparticles were made with MCF-7 breast tumor cells cultured in a 96-well plate. Figures 5a and 5b show the results obtained.
Silver and silver-iron nanoparticles did not show high toxicity with volumes of 5, 10 and 20 µL of nanoparticles. The toxicity increased with the increase in the nanoparticles volumes and ALA:AgFeNPs was more toxic than ALA:AgNPs.

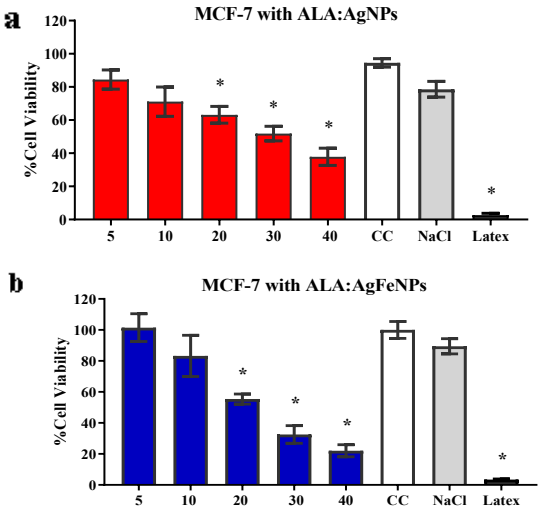

Fig. 5. Cell viability test in MCF-7 cells, incubated for 24 hours with: (a) silver nanoparticles and (b) silver-iron nanoparticles. Data were compared using the ANOVA test followed by the Dunnett test, with p *<0.001.

For prostate tumor cells, the results indicated that silver-iron nanoparticles were much more toxic than silver nanoparticles as showed in the Figures 6 a and b.

Iron is metabolized by cells allowing the easier deliver of the silver nanoparticles into the cells, which once inside the cells are toxic and lead to cell death.

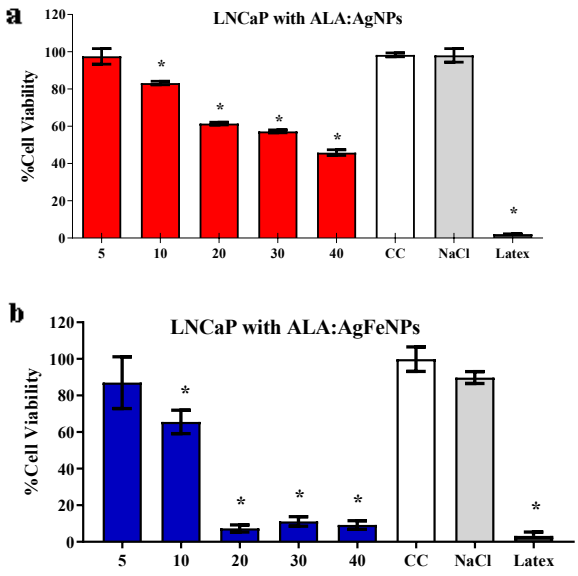

Fig. 6. Cell viability test in LNCaP cells, incubated for 24 hours with: (a) silver nanoparticles and (b) silver-iron nanoparticles. Data were compared using the ANOVA test followed by the Dunnett test, with p* <0.001.

III. CLONCLUSIONS

The synthesis of metallic silver and silver-ironnanoparticles was possible by the photoreduction method, a simple, safe, cost effective and eco friendly approach. The ALA was incorporated into the surface of the nanoparticles,

by binding of the metal with its carboxyl functional group, and its delivery was evaluated. Iron silver nanoparticles were more toxic to the breast cancer and prostate cancer cell lines evaluated. ALA:AgFeNPs induces ROS generation inside cells, carrying the ALA, which was converted to PpIX after 24 hours.

ACKNOWLEDGMENT

To the Multiuser Center of Universidade Federal do ABC (UFABC) for the support, and Multiuser Center of the Center Nuclear Fuel (IPEN/CNEN-SP) and to Fapesp (Fundação de Amparo à Pesquisa do Estado de São Paulo) grants 2014-06960-9 and 2017/23686-6)

REFERENCES

[1] X. Chen, H. J. Schluesener. "Nanosilver: a nanoproduct in medical application." Toxicol Lett, vol.176, pp 1-12, 2008.

[2] Z. Chen et al. "Acute toxicological effects of copper nanoparticles in vivo." Toxicol Lett, vol. 163, Issue 2, pp 109-120, 2006.

[3] Y.Xia et al. "One-Dimensional nanostructures: synthesis, characterization, and applications." Adv. Mater. vol. 15, n. 5, pp. 353–389, 2003.

[4] C. Cataleya et al. "Unique cellular interaction of silver nanoparticles: size-dependent generation of reactive oxygen species." J. Phys. Chem. B, vol. 112, n. 43, pp, 13608-13619, 2008.

[5] P.V. Asharani, M. P. Hande, S. Valiyaveettil. "Antiproliferative activity of silver nanoparticles." BMC Cell Biol, vol. 10, pp. 65, 2009.

[6] S. M. Hussain, J. M. Frazier." Involvement of apoptosis in hydrazine induced toxicity in rat primary hepatocytes." Toxicol in Vitro, vol. 17, n. 3, pp. 343-355, 2003.

[7] N. Duran et al. "Potential use of silver nanoparticles on pathogenic bacteria, their toxicity and possible mechanisms of action." J. Braz. Chem. Soc. vol. 21, n. 6, pp. 949-959, 2010.

[8] Peng Q., Moan J., Warloe T., Nesland J.M., Rimington C. Distribution and photosensitizing efficiency of porphyrins induced by application of exogenous 5-aminolevulinic acid in mice bearing mammary carcinoma. Int. J. Cancer. 1992;52:433–443. doi: 10.1002/ijc.2910520318

[9] K.O. Gonçalves, D.P.Vieira, L.C.Courrol."Synthesis and characterization of aminolevulinic acid gold nanoparticles: Photo and sonosensitizer agent for atherosclerosis." J. Lumin. vol. 197, pp. 317-323, 2018.

[10] L. C Courrol, F. R. de Oliveira Silva, L. Gomes. "A simple method to synthesize silver nanoparticles by photo-reduction." Colloids Surf. A vol. 305(1-3), pp. 54-5, 2007.

[11] A.Costecu, et al. "Fabrication, characterization, and antimicrobial activity, evaluation of low silver concentrations in silver-doped hydroxyapatite nanoparticles". J. Nanomater. vol. 2013, pp. 5, 2013.

[12] S.Laurent et al. "Magnetic iron oxide nanoparticles: synthesis, stabilization, vectorization, physicochemical characterizations, and biological applications." Chem. Rev. vol. 108, n. 6, pp. 2064-2110, 2008.

[13] C.Levard et al. "Environmental transformations of silver nanoparticles: impact on stability and toxicity." Environ. Sci. Technol. vol. 46, n. 13, pp. 6900-6914, 2012.

[14] N. Merclin, P. Beronius. "Transport properties and association behaviour of the zwitterionic drug 5-aminolevulinic acid in water: A precision conductometric study." Eur. J. Pharm. Sci., vol. 21, n. 2-3, p. 347-350, 2004.

[15] V.Pradeepa, T. Sriran, M. Sujatha. "Studies on drug delivery efficacy of silver nanoparticles synthesized using human serum albumin as tamoxifen carriers in MCF-7 cell line." Int J Sci Res, vol. 6, pp. 1881-1888, 2017.

[16] L.Wei et al. "Silver nanoparticles: synthesis, properties, and therapeutic applications." Drug Discov Today, vol. 20, n. 5, pp. 595-601, 2015.

[17] Q. Ding et al. "Shape-controlled fabrication of magnetite silver hybrid nanoparticles with high performance magnetic hyperthermia." Biomaterials, vol. 124, pp. 35-46, 2017.